Xenobiotica
the fate of foreign compounds in biological systems

ISSN: (Print) (Online) Journal homepage: https://www.tandfonline.com/loi/ixen20

Absorption, metabolism, and excretion of [^{14}C]-sebetralstat (KVD900) following a single oral dose in healthy male participants

Peter Mutch, Mohammad Bashir, Bonnie Jung, Ping Yi & Matt Iverson

To cite this article: Peter Mutch, Mohammad Bashir, Bonnie Jung, Ping Yi & Matt Iverson (2022): Absorption, metabolism, and excretion of [^{14}C]-sebetralstat (KVD900) following a single oral dose in healthy male participants, Xenobiotica, DOI: 10.1080/00498254.2022.2132187

To link to this article: https://doi.org/10.1080/00498254.2022.2132187

XENOBIOTICA
https://doi.org/10.1080/00498254.2022.2132187

Taylor & Francis
Taylor & Francis Group

RESEARCH ARTICLE

OPEN ACCESS Check for updates

Absorption, metabolism, and excretion of [^{14}C]-sebetralstat (KVD900) following a single oral dose in healthy male participants

Peter Mutch[a], Mohammad Bashir[b], Bonnie Jung[b], Ping Yi[b] and Matt Iverson[c]

[a]KalVista Pharmaceuticals, Salisbury, UK; [b]Labcorp Drug Development, Madison, WI, USA[c]KalVista Pharmaceuticals, Cambridge, MA, USA

ABSTRACT

1. Sebetralstat is an investigational oral plasma kallikrein inhibitor for the on-demand treatment of hereditary angioedema. Six healthy male participants received one dose of 600 mg (540 μCi) [^{14}C]-sebetralstat. Plasma concentrations of sebetralstat and levels of total radioactivity in plasma, urine, and faeces were determined. Metabolite profiles of radioactivity were generated, and major metabolites structurally characterised.
2. Radioactivity was rapidly absorbed and was excreted with a mean of 95.8% (63.4% faeces; 32.4% urine) recovered by 216 h. Sebetralstat was the major drug-related component in urine and faeces, although metabolism predominated overall (main metabolites: M19 (des-[methoxy-fluoromethylpyridine]-sebetralstat), M10 (*N*-des-pyridone-sebetralstat-carboxylic acid), M3 (pyridine *O*-desmethyl-sebetralstat), and M34 (pyridine dioxy-dihydro-sebetralstat)). Sebetralstat was the main radiolabelled component in plasma (mean of 64.1% of the total radioactivity AUC_{0-24}), followed by relatively low proportions of metabolites: M19 (7.10%), M3 (4.01%), and M10 (4.00%). Although M19 was >10% of the plasma radioactivity AUC_{0-24}, in one participant it comprised a mean of <10% of AUC_{0-24}. Plasma levels of M19 were measured at the NOAEL dose in a rat toxicology study, where higher exposure was observed *vs.* that in humans.
3. Given these findings and the lack of pharmacological activity of M19, it was concluded that there was no unique or disproportionate circulating metabolite in humans.

ARTICLE HISTORY
Received 18 July 2022
Revised 29 September 2022
Accepted 30 September 2022

KEYWORDS
Drug absorption; drug excretion; drug metabolism; hereditary angioedema; plasma kallikrein inhibitor; sebetralstat

Introduction

Hereditary angioedema (HAE) is a rare and potentially life-threatening genetic disease characterised by unpredictable tissue swelling due to an increase in vascular permeability (Maurer et al. 2018; Banday et al. 2020; Busse and Christiansen 2020). HAE attacks are commonly painful, debilitating, and typically affect the extremities, bowel mucosa, genitals, face, and upper airways (Longhurst and Cicardi 2012).

Patients with HAE types 1 and 2 have genetic abnormalities in *SERPING1* that lead to C1 inhibitor (C1-INH) deficiency (Drouet et al. 2022). C1-INH is the primary physiological inhibitor of plasma kallikrein (PKa), and decreased C1-INH in HAE leads to the dysregulation of PKa and increased generation of bradykinin, vascular permeability, and oedema (Kaplan and Joseph 2014; Busse and Christiansen 2020). HAE attacks occur when uncontrolled PKa cleaves high-molecular-weight kininogen (HK) to generate bradykinin, which signals through the bradykinin B2 receptor, resulting in vascular hyperpermeability (Kaplan 2014).

Guidelines recommend that people living with HAE should always have access to medications for on-demand treatment of HAE attacks and should treat attacks as early as possible (Maurer et al. 2018). Currently available on-demand treatments for HAE require either subcutaneous or intravenous administration, which presents a significant treatment burden due to the time needed for medication preparation and administration, challenges with vascular access, associated pain and discomfort, and infusion- or injection-site reactions (Nicola et al. 2019; Busse and Christiansen 2020). The development of an oral, rapid-acting, well-tolerated, on-demand treatment for HAE remains an unmet need.

Sebetralstat (KVD900) is a novel investigational oral plasma kallikrein inhibitor for the on-demand treatment of HAE (Duckworth et al. 2022; Maetzel et al. 2022). In a phase 1 trial of healthy adult participants, 600 mg of sebetralstat was rapidly absorbed following oral administration, with measurable plasma concentrations detected within 10–20 min post-dose (Maetzel et al. 2022). In individuals living with HAE, orally administered sebetralstat achieved rapid and near-complete *ex vivo* inhibition of PKa activity in plasma and provided rapid protection of HK from cleavage, demonstrating a close relationship between plasma concentration of sebetralstat and its effect (Duckworth et al. 2022).

CONTACT Peter Mutch peter.mutch@kalvista.com KalVista Pharmaceuticals, Ltd., Porton Science Park, Bybrook Rd, Porton Down, Wiltshire, SP4 0BF, UK
Supplemental data for this article is available online at https://doi.org/10.1080/00498254.2022.2132187

These data suggest that sebetralstat has properties that could rapidly halt HAE attacks.

Characterisation of the absorption, metabolic fate, and excretion of a drug candidate is required as part of the drug development process (US Food and Drug Administration 2010). This is generally achieved through the administration of an appropriately radiolabelled version of the drug candidate, enabling the determination of the main clearance routes and identification of any major metabolites that might require further safety assessment in line with regulatory guidelines (US Food and Drug Administration 2020). This information may also be used in the assessment of the drug–drug interaction potential of the drug candidate (US Food and Drug Administration 2010), and the routes of excretion and extent of metabolism help define the requirement for further investigation of the impact of hepatic or renal impairment. Comparison of the biotransformation profile in humans with that in toxicology species allows confirmation of the metabolic suitability of the species used in non-clinical safety testing. If major circulating metabolites are observed in humans, these can be quantified in safety species to establish the exposure margins (US Food and Drug Administration 2020).

In this trial, the absorption, metabolism, and excretion (AME) of sebetralstat were evaluated following a single oral administration of 600 mg of [^{14}C]-sebetralstat in healthy human participants. Plasma levels of the most abundant human plasma metabolite (M19 [des-(methoxy-fluoro-methyl-pyridine)-sebetralstat]; KV124020) were also measured in plasma from rats after repeated oral dosing to establish relative systemic exposures.

Materials and methods

Study design

This was a phase 1, open-label, non-randomised, single-dose trial performed at a single research centre in Madison, WI, USA. Following a 28-day screening period, participants were admitted to the clinical research unit the day before dosing (day −1) and remained in the clinical research unit for the duration of the observation period.

Ethics statement

This trial was performed in accordance with the ethical principles stated in the Declaration of Helsinki, the International Council for Harmonisation for Good Clinical Practice, and all local applicable laws and regulations, and the protocol was approved by the Institutional Review Board. Before participation, all participants signed a written informed consent form with details of the trial treatment, procedures, and potential risks.

Study population

Healthy male adults (aged 18–55 years) of any race were eligible to participate in the trial. Use of tobacco- or nicotine-containing products was prohibited within 3 months of the start of the trial and for the duration of the trial, and caffeine and alcohol consumption was similarly restricted for 48 h before check-in and during the study. Six adults were enrolled in the trial. The mean age of participants was 35.5 (*SD*, 11.67) years. Five (83.3%) participants were White, and one (16.7%) participant was Black/African American; three participants (50%) were Hispanic or Latino. The mean body weight was 83.1 (*SD*, 4.24) kg, and the mean body mass index was 27.6 (*SD*, 1.8) kg/m^2. All six participants received the study treatment, and five participants completed the study, two of whom met discharge criteria on day 9, and three who met discharge criteria on day 10. One participant withdrew from the trial early by choice on day 9; this withdrawal did not impact the use of data from this participant (see Supplemental Methods: Participant disposition).

Study medication

Sebetralstat and [^{14}C]-sebetralstat were combined in solution prior to recrystallisation, so the radiolabelled and non-radiolabelled materials were equivalent in their physical characteristics. The chemical and radiochemical stability of the dose material was determined in the radio-diluted solid material. All dose preparation was performed to good manufacturing practice. On day 1 of the trial, all participants received a single oral dose of 600 mg containing ~540 μCi of [^{14}C]-sebetralstat administered in two capsules with 240 mL of room temperature water. The structure of [^{14}C]-sebetralstat and the position of the radiolabel are shown in Figure 1. The radioactive dose was established by dosimetry calculations based on quantitative whole-body autoradiography in pigmented and non-pigmented rats. The overall whole-body radiation dose in a male participant after a dose of 540 μCi was calculated to be 8.08 and 8.35 mrem (based on data from albino and pigmented rats, respectively), well below

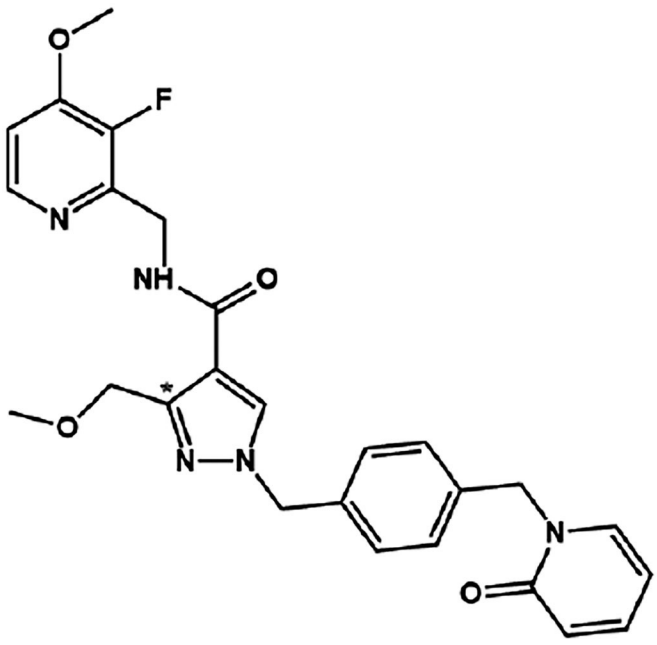

Figure 1. Structure of [^{14}C]-sebetralstat and position of radiolabel. *Indicates the position of the radiolabel.

the US Food and Drug Administration exposure limit of 3000 mrem after a single dose for human isotope studies (per 21 Code of Federal Regulations 361). During the trial, participants received a standardised high-fibre diet at scheduled times. All participants fasted overnight (≥10 h) and refrained from water for 1 h before dosing and 2 h post-dose.

Sample collection

Blood samples were collected pre-dose and at 0.25, 0.5, 1, 2, 3, 4, 5, 6, 8, 10, 12, 24, 36, and 48 h post-dose, and then every 24 h until discharge for assessments of total radioactivity in whole blood and plasma for sebetralstat concentration in plasma and for metabolite profiling and identification in plasma. Urine and faeces were analysed for total radioactivity and metabolite profiling and identification. Urine collection was performed pre-dose, and then at predefined intervals post-dose at 0–4, 4–8, 8–12, 12–24, 24–48 h, and then daily until discharge. Faeces were collected pre-dose and during the post-dose intervals 0–24 h, 24–48 h, and then daily until discharge.

Determination of total radioactivity

Levels of total radioactivity in individual plasma and urine samples were determined by weighing duplicate aliquots and were analysed by liquid scintillation counting (LSC). Individual faeces samples were homogenised in water:acetonitrile (ACN) 1:1, v/v, and duplicate weighed aliquots were combusted and analysed by LSC. Duplicate weighed aliquots of blood were combusted and analysed by LSC.

Determination of levels of sebetralstat in plasma

Levels of sebetralstat in plasma samples were measured using a validated liquid chromatography-tandem mass spectrometry assay with positive TurbolonSpray (York Bioanalytical Solutions, York, UK) ionisation and a calibration range of 1–1000 ng/mL (see Supplemental Methods: Analysis of sebetralstat concentrations in plasma).

Sample preparation for metabolite profiling and identification

Plasma samples were prepared for each participant using a time-weighted pooling method to generate area under the curve (AUC) from 0 to 24 h (AUC_{0-24}) representative pooled samples (Hop et al. 1998). Interparticipant timepoint pools were prepared for plasma samples collected at 0.5, 1, 4, 12, and 24 h by combining an equal volume of plasma from each participant. Plasma was prepared for metabolite profiling by solvent extraction in ACN and methanol (MeOH), followed by solid phase extraction (see Supplemental Methods: Sample preparation for metabolite profiling).

Individual urine samples were pooled by weight for each participant to generate 0- to 48-h pooled samples containing a mean of >97% of the radioactivity excreted *via* urine. A 1-mL subsample of each pooled urine sample was centrifuged before analysis (see Supplemental Methods: Sample preparation for metabolite profiling).

Faeces sample homogenates collected from participants over 0–24, 24–48, 48–72, 72–96, 96–120, and 120–144 h were pooled by the participant to generate pooled samples for each individual containing a mean of >98% of the radioactivity excreted *via* faeces. Faecal homogenate pools were prepared for metabolite profiling by solvent extraction in ACN and MeOH (see Supplemental Methods: Sample preparation for metabolite profiling).

Metabolite profiling and characterisation

Urine and extracts of plasma and faeces were analysed by liquid chromatography-high resolution mass spectrometry (LC-HRMS). LC flow was split, with 15% going to the mass spectrometer for metabolite characterisation and 85% to fraction collection to generate radioprofiles. Fractions were collected at 10-s intervals into 96-well plates containing solid scintillant. Radioactivity in each fraction was determined using MicroBeta2 analysis, and radiochemical profiles were generated based on radioactivity counts.

Metabolite characterisations were conducted on a Thermo Fisher Scientific Q Exactive mass spectrometry instrument. The cut-off for identification of metabolites was 1% of the sample radioactivity for plasma and 1% of the radioactive dose for urine and faeces. Characterisation of metabolites was based on mass spectrometry fragmentation patterns and comparison with an authentic reference standard of sebetralstat (see Supplemental Methods: Metabolite profiling methodology for further information).

Pharmacokinetic evaluation

Pharmacokinetic (PK) parameters for sebetralstat, total radioactivity and metabolites in plasma, and total radioactivity in blood were calculated. The maximum observed concentration (C_{max}) and time to C_{max} (T_{max}) were obtained by visual inspection of the raw data. PK parameters calculated included half-life ($t_{1/2}$), AUC from time 0 to the last measurable timepoint (AUC_{0-t}), and AUC from time 0 to infinity ($AUC_{0-\infty}$). PK parameters were calculated with Phoenix WinNonlin, version 8.1 (Pharsight Corporation, Mountainview, CA, USA).

Safety measurements

Safety was monitored from the time the participant signed the informed consent form until discharge. All adverse events (AEs) were recorded whether reported by the participant voluntarily or upon questioning or noted at the physical examination. For clinical laboratory examinations, participants fasted overnight before the collection of blood samples. Clinical chemistry, haematology, and urinalysis were performed on day 2. Vital signs were collected pre-dose, 4 h post-dose, on day 2, and on day 3. A 12-lead electrocardiogram was performed at pre-dose and 4 h post-dose

assessments. All AEs were coded using the Medical Dictionary for Regulatory Activities Version 22.1.

Statistical analyses

Mass balance and PK data were summarised with descriptive statistics, and no inferential statistical analyses were performed. The all-participant population consisted of all participants who signed the informed consent form and had any study assessment recorded in the database. The safety population consisted of all participants who received a dose of study treatment ([^{14}C]-sebetralstat). The PK population consisted of participants dosed with [^{14}C]-sebetralstat who had evaluable PK data. Each of these study populations included all six participants who received treatment.

Pharmacokinetic evaluations in rats

The PK of the most abundant human plasma metabolite M19 (KV124020) was determined in rats using repeat dose plasma samples from male and female rats dosed with sebetralstat at 300 mg/kg/day for 177 days in a 26-week toxicity study. Blood samples were collected from three animals/sex/timepoint in a composite profile pre-dose and at nominal timepoints of 0.5, 1, 2, 4, 6, 12, and 24 h post-dose. Plasma was separated and M19 was quantified using a qualified plasma assay. PK parameters by sex were generated using composite plasma concentrations of M19. This study was carried out in accordance with the UK Animals (Scientific Procedures) Act 1986 and after an ethical review process.

Results

Pharmacokinetics and excretion of [^{14}C]-sebetralstat and total radioactivity

PK parameters are presented in Table 1. In plasma, [^{14}C]-sebetralstat was rapidly absorbed in the systemic circulation, with a median sebetralstat T_{max} of 0.5 (range, 0.5–3.0) h. The geometric mean sebetralstat C_{max} was 5890 ng/mL (coefficient of variation [CV%], 35.1%), from which plasma concentrations declined in a biphasic manner. The geometric mean $t_{1/2}$ was 5.79 (range, 3.78–13.9) h (CV, 60.6%).

Maximal levels of total radioactivity occurred rapidly in plasma and whole blood, with a median T_{max} of 0.750 h post-dose in both plasma and whole blood (range, 0.500–3.00 and 0.500–3.00 h, respectively; Figures 2 and 3). The geometric mean total radioactivity C_{max} in plasma and whole blood was 8030 ng eq/mL (CV%, 35.4%) and 5380 ng eq/mL (CV%, 33.7%), respectively. Total radioactivity levels in whole blood and plasma were quantifiable in all participants up to 24 and 96 h post-dose, respectively. The $t_{1/2}$ of total radioactivity was longer in plasma than that of the parent compound (136 and 5.79 h, respectively); the $t_{1/2}$ of total radioactivity in the whole blood was 10.3 h (which may be limited by the lower sensitivity of quantification of radioactivity in blood compared with plasma). Together with the observation that the $AUC_{0-\infty}$ plasma sebetralstat/total radioactivity ratio was 0.409, these findings indicate that radiolabelled metabolites circulate in the plasma after administration of [^{14}C]-sebetralstat. The mean whole blood/plasma ratio for total radioactivity at timepoints between 0.25 and 24 h ranged from 0.596 to 0.670, which indicated that there was little radioactivity associated with blood cells.

A summary of the cumulative total radioactivity recovered from excreta is shown in Table 2 (detailed timepoint data are shown in Supplemental Table 1). Cumulative excretion is shown in Figure 4. By 216 h post-dose, the overall mean recovery of total radioactivity was 63.4% in faeces and 32.4% in urine, resulting in 95.8% overall (range in individual participants, 87.0–99.7%). Urine and faecal samples collected during the first 96 h post-dose accounted for a mean radioactivity recovery of 90.2% of the administered dose. Levels of urinary total radioactivity were below the limit of quantification in four of the six participants by 192 h post-dose. Faecal samples contained quantifiable levels of radioactivity through the discharge in all participants. The intervals with the greatest proportion of total radioactivity recovered were 0–4 h for urine samples and 24–48 h for faeces samples.

Structure elucidation of metabolites

The major metabolites observed in plasma, urine, and faeces are shown in Table 3. Representative radiochromatograms of plasma, urine, and faeces are shown in Figure 5. Proposed metabolite assignment, molecular ion, molecular formula, and characteristic product ions of these major metabolites

Table 1. Summary of pharmacokinetic parameters for sebetralstat following oral dosing of [^{14}C]-sebetralstat.

Pharmacokinetic parameter	Plasma sebetralstat	Plasma total radioactivity	Whole blood total radioactivity
$AUC_{0-\infty}$ (ng·h/mL)[a]	17 500 (37.2) [6]	49 300 (22.4) [3]	22 800 (16.8) [6]
AUC_{0-last} (ng·h/mL)[a]	17 400 (37.2) [6]	40 900 (19.0) [6]	21 200 (19.1) [6]
$\%AUC_{extrap}$ (%)	0.123 (364.4) [6]	10.8 (58.5) [3]	6.23 (55.4) [6]
C_{max} (ng/mL)[a]	5890 (35.1) [6]	8030 (35.4) [6]	5380 (33.7) [6]
T_{max} (h)	0.500 (0.500–3.00) [6]	0.750 (0.500–3.00) [6]	0.750 (0.500–3.00) [6]
T_{last} (h)	42.0 (36.0–72.0) [6]	168 (120–192) [6]	30.0 (24.0–48.0) [6]
$t_{1/2}$ (h)	5.79 (60.6) [6]	136 (120.9) [5]	10.3 (44.6) [6]
$AUC_{0-\infty}$ plasma sebetralstat/total radioactivity ratio[b]	N/A	0.409 (16.5) [3]	N/A

Geometric mean (CV) [*n*] is presented for all variables except T_{max} and T_{last}, for which median (range) [*n*] is presented.
AUC: area under the concentration-time curve; $AUC_{0-\infty}$: AUC from time 0 extrapolated to infinity; AUC_{0-last}: AUC from time 0 to the time of the last quantifiable concentration (T_{last}); $\%AUC_{extrap}$: percentage of AUC due to extrapolation from the last quantifiable concentration to infinity; C_{max}: maximum observed concentration; CV: coefficient of variation; h: hour; *n*: number of participants with valid observations; N/A: not applicable; $t_{1/2}$: apparent terminal elimination half-life; T_{last}: time to last observed concentration; T_{max}: time to C_{max}.
[a]Units for total radioactivity AUCs and C_{max} are ng equivalents·h/g and ng equivalents/g, respectively.
[b]$AUC_{0-\infty}$ of sebetralstat in plasma relative to $AUC_{0-\infty}$ of total radioactivity in plasma.

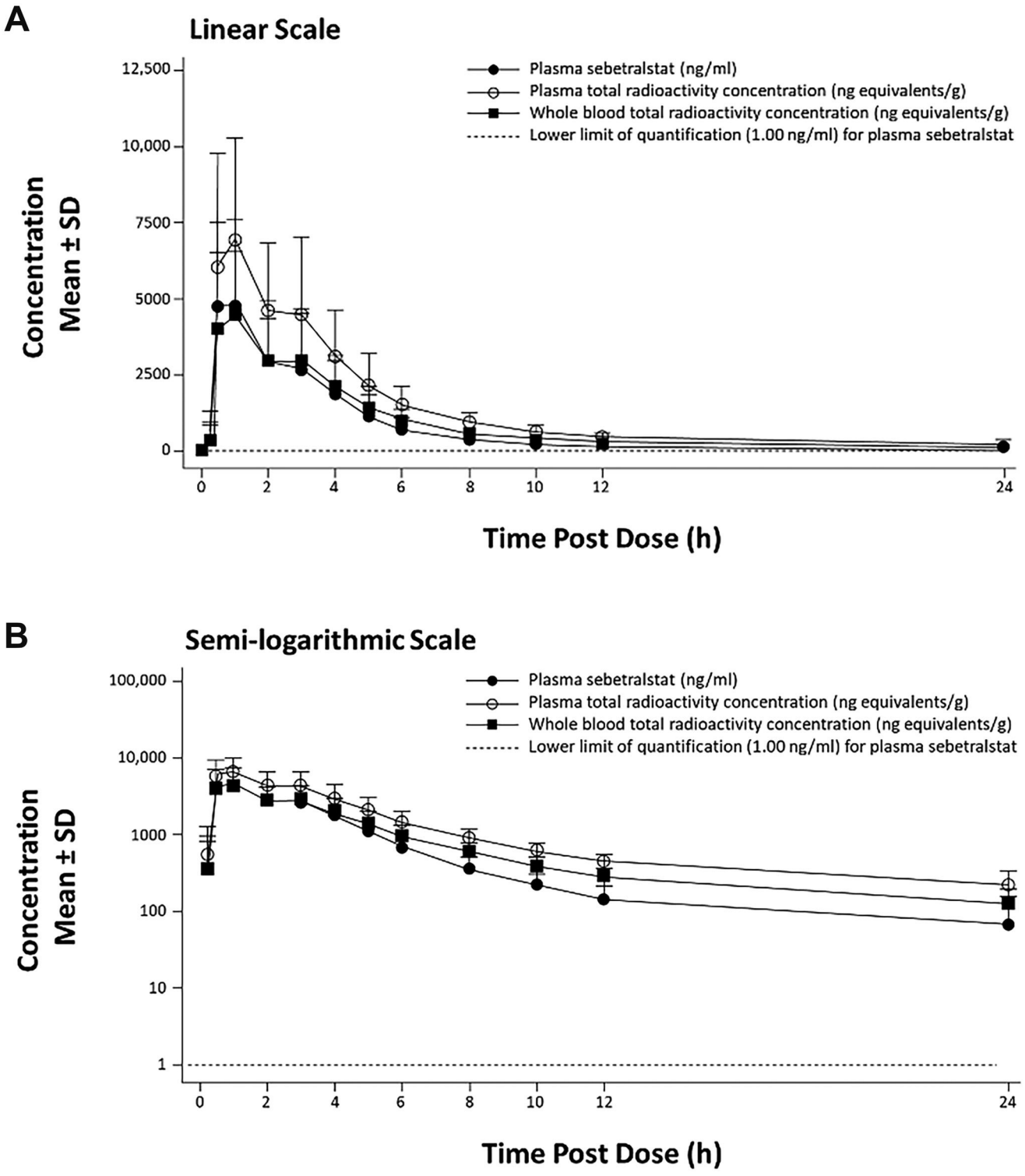

Figure 2. Arithmetic mean concentrations of sebetralstat in plasma and total radioactivity in plasma and whole blood following oral dosing of [^{14}C]-sebetralstat on a linear scale (A) and semi-logarithmic scale (B) for up to 24 h. h: hour.

are shown in Table 4 (see Supplemental Figure 1 for the proposed structures and fragmentation patterns for each metabolite).

Plasma

Analysis of AUC-pooled and timepoint–pooled plasma samples with LC-HRMS characterised 11 metabolites. Biotransformation occurred at different points in the molecule, including *via* chain cleavage. Sebetralstat was the predominant component in plasma, accounting for a mean of 64.1% of the total radioactivity in $AUC_{0–24}$ pooled samples.

The main plasma metabolites (representing a mean of $\geq$2% of the total radioactivity in $AUC_{0–24}$ pooled samples) were M19 (des-[methoxy-fluoro-methylpyridine]-sebetralstat; 7.10%), M10 (*N*-des-pyridone-sebetralstat-carboxylic acid; 4.00%), and M3 (pyridine *O*-desmethyl-sebetralstat;

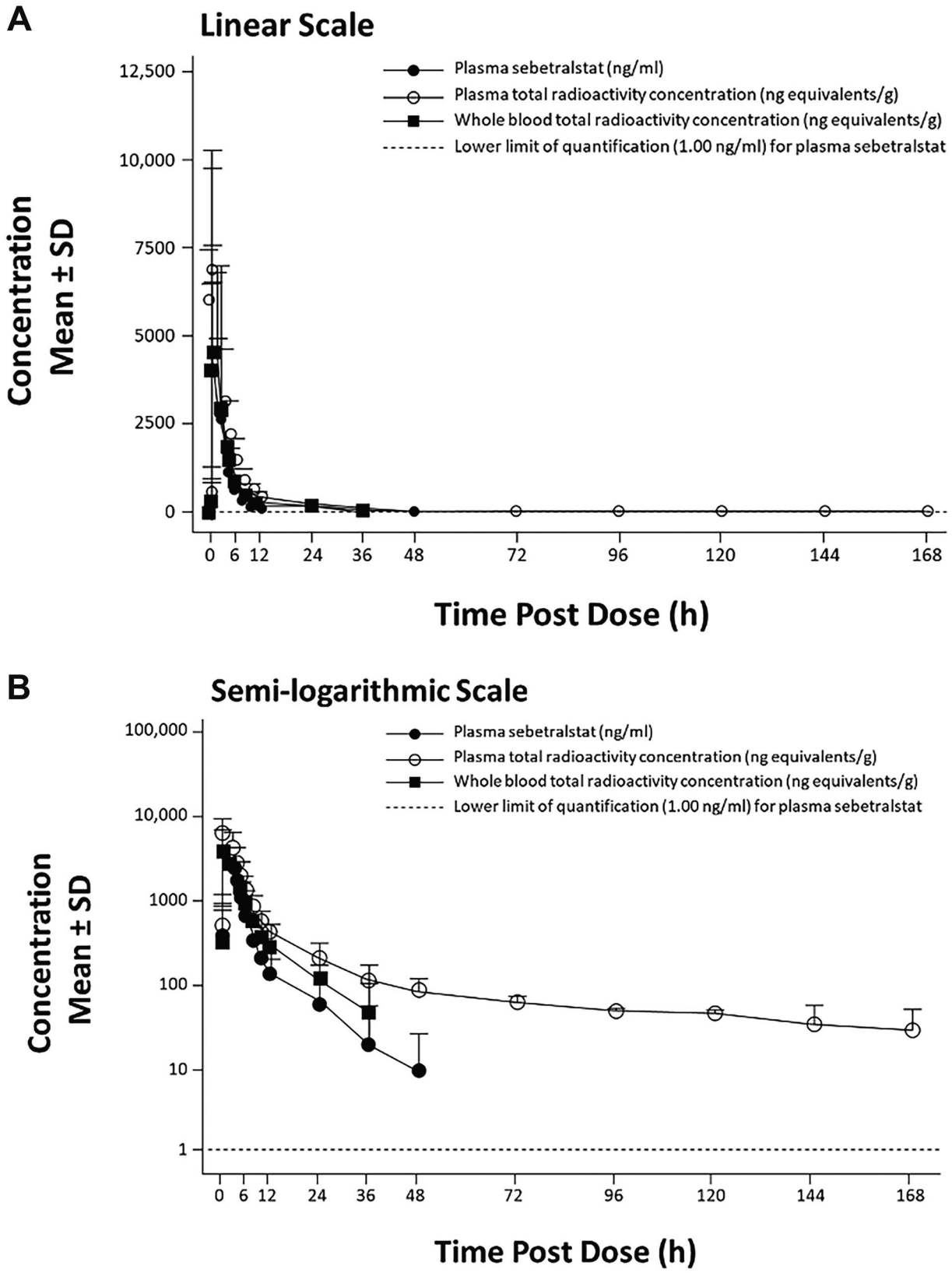

Figure 3. Arithmetic mean concentrations of the full profile of sebetralstat in plasma and total radioactivity in plasma and whole blood following oral dosing of [^{14}C]-sebetralstat on a linear scale (A) and semi-logarithmic scale (B) (N = 6). Plots include timepoints where at least three participants had a quantifiable value for the respective analyte. h: hour.

4.01%) (Table 3). In individual participants, metabolite M19 represented a range of 5.42–10.55 of the total radioactivity in the AUC_{0-24} pools, with a mean AUC_{0-24} of 2270 ng equivalents·h/g. By 24 h post-dose, only sebetralstat was detectable as a distinct peak in plasma by radio-high-performance liquid chromatography. All plasma metabolites observed are tabulated in Supplemental Table 2.

Urine

Excretion *via* urine eliminated 32% of the radioactive dose, with unchanged sebetralstat present as the most abundant drug-related component (mean of 8.66% of the dose; range 4.20–12.9% across participants). Sebetralstat and 15 metabolites were characterised in urine samples using LC-HRMS. The most abundant metabolites in the urine were M19 and M10/M41 (coeluting; M41 is pyridine dioxy-dihydro-sebetralstat), with means of 4.21% and 4.88% of the dose, respectively. Metabolites that composed a mean of 2–3% of the dose were M3 (2.55%) and M34 (pyridine dioxy-dihydro-sebetralstat; 2.95%). Two unidentified urinary trace metabolites were also observed. All urinary metabolites observed are tabulated in Supplemental Table 3.

Table 2. Cumulative percentage of radioactive dose recovered in urine and faeces (mean ± *SD*; $N = 6$).

Interval (h)	Urine	Faeces	Total
0–24	30.0 ± 8.06	7.81 ± 16.5	37.8 ± 21.3
0–96	32.3 ± 6.60	57.9 ± 7.93	90.2 ± 11.0
0–216	32.4 ± 6.57	63.4 ± 3.59	95.8 ± 5.02

For detailed timepoint data, refer to Supplemental Table 1. h: hour.

Faeces

Most [^{14}C]-sebetralstat-related radioactivity was excreted in faeces, with 63% of the administered dose recovered via this route. Sebetralstat and 13 metabolites were characterised in faeces using LC-HRMS. A further 13 metabolites were unidentified, each of which represented a mean of <1% of the

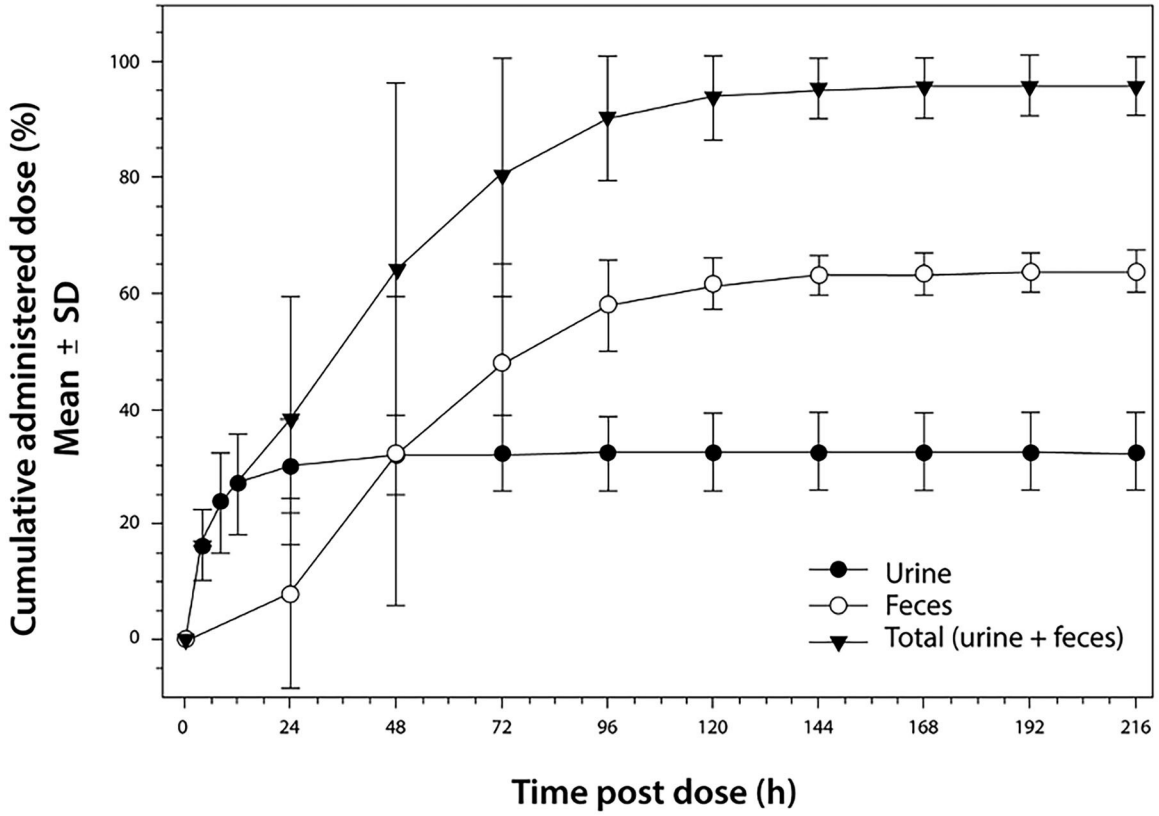

Figure 4. Cumulative percent of radioactive dose recovered in urine and faeces at specified intervals following oral dosing of [^{14}C]-sebetralstat. h: hour.

Table 3. Major metabolites detected in human plasma, urine, and faeces following oral dosing of [^{14}C]-sebetralstat (mean ± *SD*; $N = 6$).

Metabolite		Plasma[a] % AUC_{0-24}	Urine[a] % dose	Faeces[a] % dose
M3	Pyridine *O*-desmethyl-sebetralstat	4.01 ± 1.45	2.55 ± 0.641	8.16 ± 1.33
M6	Pyrazole *O*-desmethyl-sebetralstat	0.765 ± 0.284	0.732 ± 0.341	1.38 ± 0.385[b]
M10	*N*-des-pyridone-sebetralstat-carboxylic acid	4.00 ± 1.44	4.88 ± 1.13[c]	1.84 ± 0.759
M19	Des-[methoxy-fluoro-methylpyridine]-sebetralstat	7.10 ± 2.03	4.21 ± 0.653	0.783 ± 0.335
M34	Pyridine dioxy-dihydro-sebetralstat	1.06 ± 0.239	2.95 ± 0.750	8.32 ± 2.88
M38/M39	Coeluting pyridine dioxy-dihydro-sebetralstat (M38) and oxidised pyrazole *O*-desmethyl-sebetralstat (M39)	1.79 ± 0.700	1.21 ± 0.430	2.68 ± 0.758
M40	Oxy-sebetralstat	Not detected	1.24 ± 0.332	2.88 ± 0.886
Sebetralstat	—	64.1 ± 8.60	8.66 ± 3.40	12.5 ± 8.86
Other characterised peaks	—	2.74	2.56	3.35
Unidentified minor/trace peaks	—	14.4	0.35	6.35

AUC_{0-24}: area under the concentration-time curve from hour 0 to 24.
[a]Timepoints for sample pooling are described in Materials and Methods.
[b]M6 coeluted with a dioxy-tetrahydro-sebetralstat product (M35) in faeces.
[c]M10 coeluted with a dioxy-dihydro-sebetralstat product (M41) in urine.

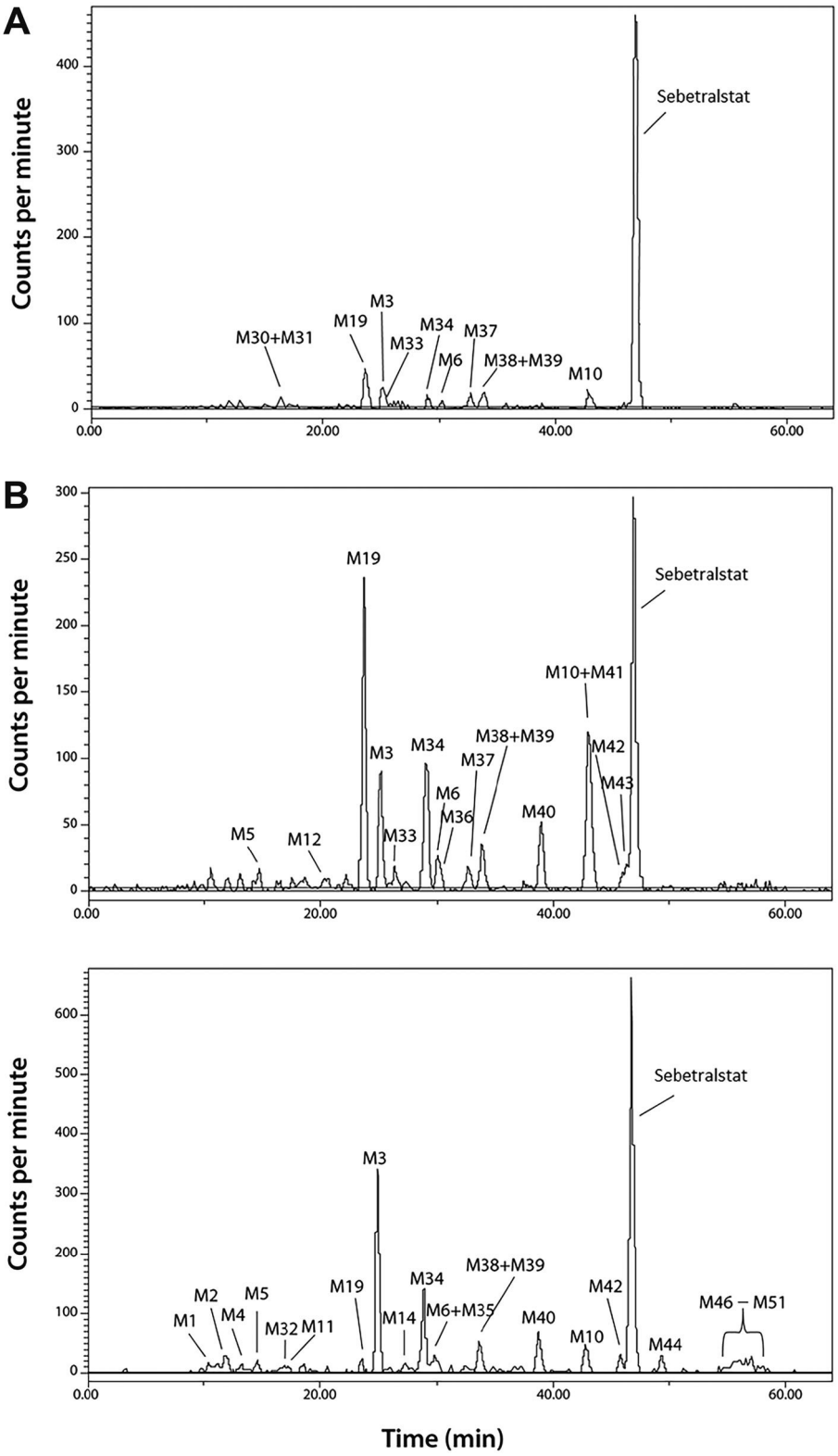

Figure 5. Radiochromatograms from analyses of AUC-pooled samples of plasma (0–24 h post-dose) (A), urine (0–48 h post-dose) (B), and faeces (0–144 h post-dose) (C) after a single oral dose of [^{14}C]-sebetralstat in representative male participants (600 mg, 540 μCi). AUC: area under the concentration-time curve; h: hour; min: minute.

dose. Based on radio-high-performance liquid chromatography profiles, a mean of ~12.5% of the total radioactivity was present as unchanged sebetralstat (range, 3.02–24.1% across participants); the two most abundant metabolites were M34 (8.32% of dose) and M3 (8.16% of dose). Other components that composed a mean of >2% of the dose in faeces were M40 (oxy-sebetralstat; 2.88%) and coeluting M38/M39 (pyridine dioxy-dihydro-sebetralstat/oxidised

Table 4. Mass spectral analysis of major metabolites of sebetralstat in human plasma, urine, and faeces.

Metabolite no.	Biotransformation route	$[M+H]^+$ (*m/z*)	Elemental composition	Characteristic fragment ions (*m/z*)
Sebetralstat		492	$C_{26}H_{27}FN_5O_4^+$	460, 442, 354, 336, 304, 198, 158, 104, 96, 78
M3	Pyridine *O*-desmethylation	478	$C_{25}H_{25}FN_5O_4^+$	446, 428, 354, 336, 304, 198, 144, 104
M6	Pyrazole *O*-desmethylation	478	$C_{25}H_{25}FN_5O_4^+$	460, 442, 322, 227, 198, 158, 157, 104
M10	*N*-dealkylation of pyridine moiety followed by oxidation	429	$C_{21}H_{22}FN_4O_5^+$	397, 273, 158, 135, 107, 91
M19	*N*-dealkylation	353	$C_{19}H_{21}N_4O_3^+$	321, 304, 198, 104, 96
M34	Pyridine dioxidation/dihydrogenation	526	$C_{26}H_{29}FN_5O_6^+$	508, 494, 476, 458, 370, 232, 214, 158, 104
M38	Pyridine dioxidation/dihydrogenation	526	$C_{26}H_{29}FN_5O_6^+$	508, 494, 476, 458, 370, 232, 214, 158, 104
M39	Oxidation of M6	492	$C_{25}H_{23}FN_5O_5^+$	448, 310, 198, 183, 158, 104
M40[a]	Oxidation of pyridin-2(1H)-one moiety	508	$C_{26}H_{27}FN_5O_5^+$	476, 458, 370, 214, 158, 104

[a]M40 was not detected in plasma samples.

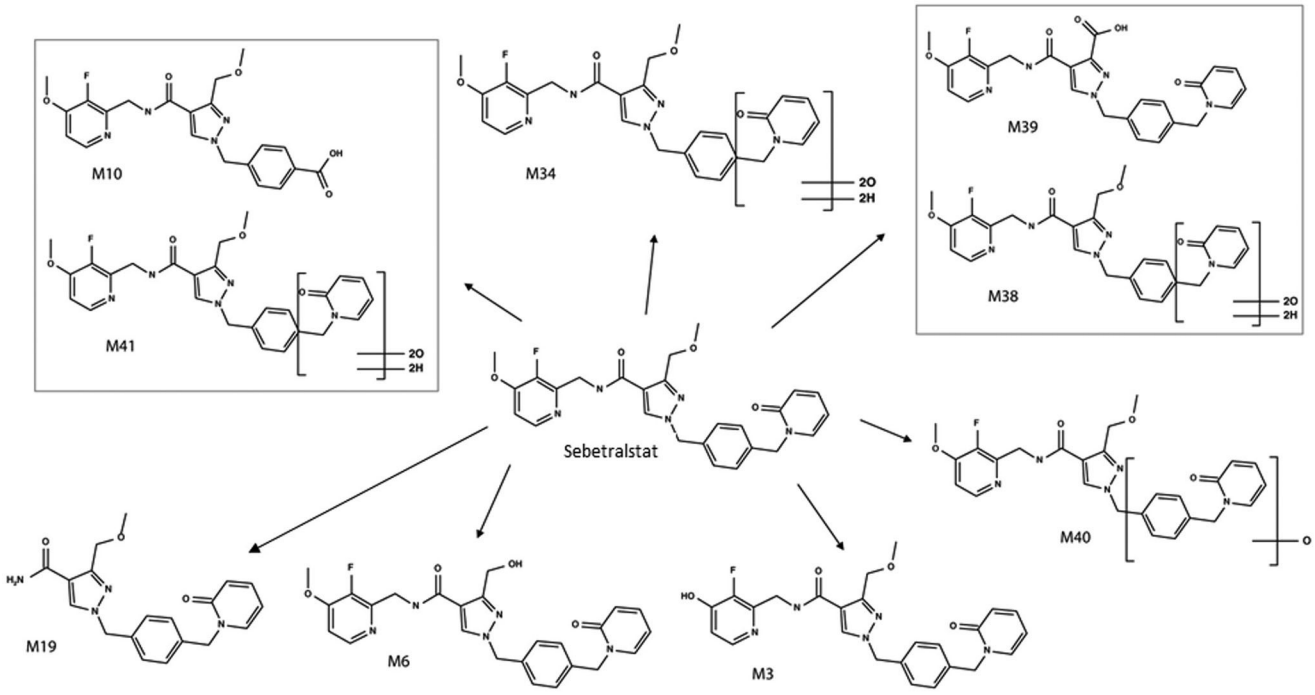

Figure 6. Major metabolites (>2% of dose excreted or >2% of AUC_{0-24} of plasma total radioactivity) detected in human urine, faeces, and plasma after oral dosing of [^{14}C]-sebetralstat. AUC_{0-24}: area under the concentration-time curve from hour 0 to 24.

Table 5. Pharmacokinetic parameters of M19 in rat plasma following daily oral gavage administration of sebetralstat at 300 mg/kg/day: day 177 of a 6-month toxicology study.

Sex	C_{max} (ng/mL)	T_{max} (h)	AUC_{0-24} (ng·h/mL)
M	792	6.0	8470
F	214	2.0	1640

AUC_{0-24}: area under the concentration-time curve from hour 0 to 24; C_{max}: maximum observed concentration; h: hour; T_{max}: time to C_{max}.

pyrazole *O*-desmethyl-sebetralstat: 2.68%). All faecal metabolites observed are tabulated in Supplemental Table 4.

Major metabolic pathways

After oral administration of [^{14}C]-sebetralstat, sebetralstat was extensively metabolised by several different routes of biotransformation. The most prevalent metabolites (those composing a mean of >2% of the total radioactivity AUC_{0-24} in plasma or >2% of the dose in excreta) are shown in Figure 6 and were formed by *N*-dealkylation (M19), *O*-desmethylation (M3; M6), oxidation (M40), *N*-dealkylation with oxidation (M10), *O*-desmethylation with oxidation (M39), and dioxidation with dihydrogenation (M34, M38, M41). Although M6 (pyrazole *O*-desmethyl-sebetralstat) composed <2% of the dose in urine and faeces individually, it was >2% in these matrices combined (although it coeluted with M35, a pyridine dioxy-dihydro-sebetralstat component, in faeces).

Comparative exposure of M19 in humans and rats

The mean percentage of the total radioactivity AUC_{0-24} for metabolite M19 was 7.10%, but it exceeded 10% (10.55%) in one participant. To compare this exposure with that at a no adverse effect level (NOAEL) of sebetralstat in rats, the rodent toxicology species, the repeat dose exposure of M19 in a 26-week, repeat-dose toxicity study in rats was determined (Table 5). After daily administration of sebetralstat at 300 mg/kg/day (the NOAEL dose), the AUC_{0-24} was 8470 ng·h/mL in males and 1640 ng·h/mL in females on day 177.

Safety

There were no deaths, serious AEs, or treatment-related AEs leading to discontinuation reported during the trial. No

clinically significant abnormalities were observed in clinical chemistry, haematology, coagulation, and urinalysis data. Vital signs and electrocardiography data were normal. One participant reported an incident of treatment-emergent diarrhoea (Grade 1) on day 6 of the trial that was deemed not related to the study drug by the investigator. No other treatment-emergent AEs were reported.

Discussion

In this phase 1, open-label, single-dose trial, radioactivity was rapidly absorbed into plasma following oral administration of [^{14}C]-sebetralstat, then excreted, with a mean of >90% of administered radioactivity recovered within 96 h and >95% recovered within 9 days. Unchanged sebetralstat was the predominant drug-related component in plasma, with only one metabolite (M19) exceeding the threshold of 10% of total radioactivity plasma AUC_{0-24} in a single participant. Clearance of sebetralstat was mainly via metabolism; sebetralstat composed only 21.2% of the dose excreted in urine (8.66%) and faeces (12.5%) combined. Extensive metabolism of [^{14}C]-sebetralstat to multiple biotransformation products, each representing relatively low proportions of dose, was observed. Metabolism occurred at several sites around the molecule, indicating no single predominant route of biotransformation. The study treatment was well-tolerated, with one Grade 1 treatment-emergent AE of diarrhoea reported and no other safety findings.

In this trial, sebetralstat demonstrated AME properties that would be beneficial for an on-demand treatment for patients with HAE. The early T_{max} of sebetralstat and of total radioactivity indicated rapid absorption in the systemic circulation. Elimination of sebetralstat occurred rapidly through extensive metabolism and excretion in both faeces and urine. Unchanged sebetralstat represented <25% of the dose in the faeces of any individual participant, which suggests that oral absorption is >75%. While intestinal biotransformation by gut flora may contribute to faecal metabolites, the major metabolites in faeces were also seen in plasma and were oxidative in nature. No direct phase 2 conjugation of sebetralstat has been observed in rats (including bile), monkeys, or humans, so cleavage of conjugated sebetralstat eliminated in bile to sebetralstat in faeces would not be likely to contribute to levels of faecally eliminated sebetralstat.

The findings indicate that metabolites of sebetralstat substantially contributed to the detected total radioactivity in the plasma, although sebetralstat itself was the main drug-related component. The notably longer terminal plasma $t_{1/2}$ of total radioactivity compared with that of sebetralstat may be due in part to radioactivity being quantifiable for longer, and in part to the possible longer $t_{1/2}$ of circulating metabolites. Given that sebetralstat was the only drug-related peak evident in the radiochromatogram of pooled plasma at 24 h, this may suggest that the circulating radioactivity at later timepoints reflects multiple components, each of low concentration and that no single significant metabolite persists. In addition, it may be that a very tight association of drug-related material with plasma proteins at later timepoints—consistent with lower solvent extraction of radioactivity from pooled plasma at 12 and 24 h (see Supplemental Material, Sample preparation for metabolite profiling, plasma, paragraph 2)—may contribute to the long half-life of total radioactivity in plasma. The geometric mean whole blood/plasma ratio for total radioactivity suggested that radioactivity had low association with blood cells in the circulation.

Although sebetralstat was the main component of the excreta (a mean of 21.2% of the dose in urine and faeces combined), this unchanged compound accounted for a relatively small proportion of the urine and faecal radioactivity. Some, or all, of the unchanged sebetralstat in faeces may be unabsorbed dose. As each individual participant excreted <13% of the dose as sebetralstat in urine, it is unlikely sebetralstat would be a victim of drug interactions caused by inhibition of renal transporters. The majority of the radioactivity was excreted as biotransformation products. The major metabolites (expressed as percentage of dose in urine and faeces combined) were M34 (pyridine dioxy-dihydro-sebetralstat; 11.3%), M3 (pyridine *O*-desmethyl-sebetralstat; 10.7%), M19 (des-[methoxy-fluoro-methyl-pyridone]-sebetralstat; 5.0%), M40 (oxy-sebetralstat; 4.1%), and M10 (*N*-des-pyridone-sebetralstat-carboxylic acid; 6.7%, although M10 coeluted with another component in urine). The metabolic fate of sebetralstat was therefore via several different routes, including chain cleavage, at different points in the molecule.

The most predominant plasma metabolite, M19, composed a mean of <10% of drug-related material in the AUC_{0-24}, but was >10% of the AUC_{0-24} in one participant. Metabolites present at >10% of total drug-related exposure at a steady state should be considered for safety assessment (US Food and Drug Administration 2020). Given that sebetralstat is intended as an intermittent on-demand treatment and will not be dosed in steady state, the M19 exposure in the [^{14}C]-sebetralstat study is considered representative of the clinical exposure at a dose of 600 mg. The mean radioactivity AUC_{0-24} of M19 was 2270 ng equivalents·h/g. Considering the relative molecular weights of sebetralstat (491.5) and M19 (352.4), and assuming 1 g = 1 mL, this equates to an M19 AUC of 1630 ng·h/mL. The repeat dose AUC_{0-24} at the NOAEL dose level in a 26-week rat toxicology study was 1640 and 8470 ng·h/mL in females and males, respectively. Given that M19 constitutes a mean of <10% of plasma AUC_{0-24} in human participants, the similar or greater exposure of M19 at the NOAEL dose in rats, the intermittent dosing of sebetralstat clinically, and the lack of pharmacological activity of M19 (IC_{50} >100 μM; data not shown), it was considered that no human plasma metabolites of sebetralstat are categorised as unique or disproportionate.

Conclusion

Rapid and extensive absorption of radioactivity was observed after a single dose of 600 mg [^{14}C]-sebetralstat in humans, followed by quantitative recovery of radioactivity in excreta, mostly by 96 h post-dose. Faecal excretion of radioactivity

was approximately double that in urine. Extensive biotransformation was seen in multiple metabolites, each of relatively low abundance. The most abundant plasma metabolite represented a mean of <10% of the total radioactivity AUC_{0-24} and was present at similar or higher levels in plasma in rats at the NOAEL dose level in a 26-week toxicology study. Good tolerability was observed during this single-dose PK trial in healthy participants, with one mild event of diarrhoea reported.

Acknowledgements

Medical writing assistance was provided under the direction of the authors by Lisa Baker, Ph.D., and Michael Howell, Ph.D., of Cadent, a Syneos Health group company, and was supported by KalVista Pharmaceuticals, Inc.

Author contributions

Mutch P. and Iverson M. participated in the research design. Bashir M., Jung B., and Yi P. conducted experiments. Mutch P., Bashir M., Jung B., Yi P., and Iverson M. performed data analysis and wrote or contributed to the writing of the manuscript.

Disclosure statement

PJM and MI are employees of KalVista Pharmaceuticals, Inc. BJ, MB, and PY have nothing to disclose.

Funding

The study was supported by KalVista Pharmaceuticals Ltd.

Data availability statement

Reasonable requests for access to data will be considered and should be addressed to the corresponding author.

References

Banday AZ, Kaur A, Jindal AK, Rawat A, Singh S. 2020. An update on the genetics and pathogenesis of hereditary angioedema. Genes Dis. 7(1): 75–83.

Busse PJ, Christiansen SC. 2020. Hereditary angioedema. N Engl J Med. 382(12):1136–1148.

Drouet C, López-Lera A, Ghannam A, López-Trascasa M, Cichon S, Ponard D, Parsopoulou F, Grombirikova H, Freiberger T, Rijavec M, et al. 2022. *SERPING1* variants and C1-INH biological function: a close relationship with C1-INH-HAE. Front Allergy. 3:835503.

Duckworth EJ, Murugesan N, Li L, Rushbrooke LJ, Lee DK, De Donatis GM, Maetzel A, Yea CM, Hampton SL, Feener EP. 2022. Pharmacological suppression of the kallikrein kinin system with KVD900: an orally available plasma kallikrein inhibitor for the on-demand treatment of hereditary angioedema. Clin Exp Allergy. 52(9): 1059–1070.

Hop CE, Wang Z, Chen Q, Kwei G. 1998. Plasma-pooling methods to increase throughput for *in vivo* pharmacokinetic screening. J Pharm Sci. 87(7):901–903.

Kaplan AP. 2014. The bradykinin-forming cascade: a historical perspective. Chem Immunol Allergy. 100:205–213.

Kaplan AP, Joseph K. 2014. Pathogenic mechanisms of bradykinin mediated diseases: dysregulation of an innate inflammatory pathway. Adv Immunol. 121:41–89.

Longhurst H, Cicardi M. 2012. Hereditary angio-oedema. Lancet. 379(9814):474–481.

Maetzel A, Smith MD, Duckworth EJ, Hampton SL, De Donatis GM, Murugesan N, Rushbrooke LJ, Li L, Francombe D, Feener EP, et al. 2022. KVD900, an oral on-demand treatment for hereditary angioedema: phase 1 study results. J Allergy Clin Immunol. 149(6): 2034–2042.

Maurer M, Magerl M, Ansotegui I, Aygoren-Pursun E, Betschel S, Bork K, Bowen T, Balle Boysen H, Farkas H, Grumach AS, et al. 2018. The international WAO/EAACI guideline for the management of hereditary angioedema: the 2017 revision and update. Allergy. 73(8):1575–1596.

Nicola S, Rolla G, Brussino L. 2019. Breakthroughs in hereditary angioedema management: a systematic review of approved drugs and those under research. Drugs Context. 8:212605.

US Food and Drug Administration. 2010. Guidance document: M3(R2) nonclinical safety studies for the conduct of human clinical trials and marketing authorization for pharmaceuticals [accessed 2022 May 13]. https://www.fda.gov/regulatory-information/search-fda-guidance-documents/m3r2-nonclinical-safety-studies-conduct-human-clinical-trials-and-marketing-authorization.

US Food and Drug Administration. 2020. Safety testing of drug metabolites: guidance for industry [accessed 2022 May 13]. https://www.fda.gov/media/72279/download.